

Neutron spin rotation in \bar{n} - d scattering

R. Schiavilla^{1,2}, M. Viviani³, L. Girlanda³, A. Kievsky³, L.E. Marcucci³

¹*Jefferson Lab, Newport News, VA 23606, USA*

²*Department of Physics, Old Dominion University, Norfolk, VA 23529, USA*

³*INFN, Sezione di Pisa, and Department of Physics, University of Pisa, I-56127 Pisa, Italy*

(Dated: August 18, 2021)

The neutron spin rotation induced by parity-violating (PV) components in the nucleon-nucleon potential is studied in \bar{n} - d scattering at zero energy. Results are obtained corresponding to the Argonne v_{18} two-nucleon and Urbana-IX three-nucleon strong-interaction potentials in combination with either the DDH or pionless EFT model for the weak-interaction potential. We find that this observable is dominated by the contribution of the long-range part of the PV potential associated with pion exchange. Thus its measurement could provide a further constraint, complementary to that coming from measurements of the photon asymmetry in \bar{n} - p radiative capture, on the strength of this component of the hadronic weak interaction.

PACS numbers: 21.30.-x, 24.80.+y, 25.10.+s, 25.40.Dn

I. INTRODUCTION

We report on a calculation of the neutron spin rotation in \bar{n} - d scattering at zero energy. The present work is the continuation of a program to study parity-violating (PV) effects in few-nucleon systems induced by hadronic weak interactions. Two earlier papers dealt with the two-nucleon systems: the first [1] was devoted to \bar{p} - p elastic scattering, and presented a calculation of the longitudinal asymmetry in the lab-energy range 0–350 MeV. The second [2] provided a detailed account of the i) neutron spin rotation in \bar{n} - p scattering at zero energy, ii) longitudinal asymmetry in \bar{n} - p elastic scattering up to lab energies of 350 MeV, iii) photon angular asymmetry in \bar{n} - p radiative capture at thermal neutron energies, and iv) photon helicity dependence of the $d(\vec{\gamma}, n)p$ cross section from threshold up to energies of 20 MeV.

In this study we adopt two different models for the PV potential. One is parameterized in terms of π -, ρ -, and ω -meson exchanges, in which the weak couplings of these mesons to the nucleon are estimated within a quark-model approach incorporating symmetry arguments and current algebra requirements. It is known as the DDH model [3], and has provided for over two decades a useful framework for the analysis and interpretation of measurements of PV observables (see in this connection the recent review in Ref. [4]).

The other model is that derived recently by Zhu *et al.* [5] in an effective field theory (EFT) approach, in which only nucleons are retained as explicit dynamical degrees of freedom, while pions and baryon resonances, such as Δ isobars, are integrated out. It is formulated in terms of a number of four-nucleon contact terms. Obviously, its use is restricted to processes occurring at energies much below the pion mass.

The rotation of the neutron spin in a plane transverse to the beam direction is calculated perturbatively to first order in the DDH and EFT PV potentials. We use n - d wave functions obtained with the hyperspherical-harmonics (HH) method [6, 7, 8] from realistic strong-interaction Hamiltonians, consisting of the Argonne v_{18} [9] (AV18) two-nucleon potential with and without the inclusion of a three-nucleon potential, the Urbana IX model [10]. The AV18/UIX Hamiltonian quantitatively and successfully accounts for a wide variety of few-nucleon bound-state properties and reactions, ranging from binding energies and charge radii to electromagnetic form factors, low-energy scattering observables and electroweak capture cross sections (for a review, see Refs. [11, 12]).

Our prime objectives in this as in the earlier papers are to develop a systematic and consistent framework for studying PV observables in few-nucleon systems, where accurate microscopic calculations are feasible, and to use available and forthcoming experimental data on these observables to constrain the strengths of the long- and short-range parts of the two-nucleon weak interaction. While no measurements of the neutron spin rotation in \bar{n} - d scattering have been carried out so far to the best of our knowledge, nevertheless we hope the present study will provide strong motivation for undertaking this type of experiments. Within the context of the calculations based on the DDH model, we find that this observable is dominated by the contribution associated with the long-range pion-exchange component. Indeed, assuming a liquid deuterium density of $\rho = 0.4 \times 10^{23}$ atoms cm^{-3} and the “best” values of Ref. [3] (as listed in Table II of Ref. [2]) for the π -, ρ -, and ω -meson weak (and strong) coupling constants to the nucleon, the predicted spin rotation per unit-length of matter traversed is 0.52×10^{-7} rad-cm $^{-1}$ with the complete DDH potential, and 0.46×10^{-7} rad-cm $^{-1}$ when only its pion-exchange term is retained. We find the model dependence of this result upon the (realistic) strong-interaction potentials used to generate the n - d continuum states to be quite small. Thus, a measurement of the \bar{n} - d spin rotation could provide a further constraint, complementary to that coming from the

measurements in progress of the photon asymmetry in the \bar{n} - p radiative capture, on the strength of the long-range part of the PV potential.

The remainder of this paper is organized as follows. In Sec. II the neutron-spin-rotation observable is related to matrix elements of the PV potential between incoming and outgoing n - d states. The DDH and EFT PV potential models are briefly discussed in Sec. III; in particular, in Appendix A it is shown that the number of independent four-nucleon contact terms in the EFT formulation is five rather than ten, as obtained in Ref. [5]. The Monte Carlo techniques used to calculate the relevant matrix elements are reviewed in Sec. IV, where the details of a test calculation based on simple Gaussian wave functions are also described. Finally, Sec. V contains a brief discussion of the results along with some concluding remarks.

II. THE NEUTRON SPIN ROTATION OBSERVABLE

In first order perturbation theory in the weak interactions, the neutron spin rotation per unit-length of matter traversed, $d\phi/dz$, in \bar{n} - d scattering is given by [2, 13]

$$\frac{1}{\rho} \frac{d\phi}{dz} = \frac{1}{3 v_{\text{rel}}} \text{Re} \sum_{m_n m_d} \epsilon_{m_n}^{(-)} \langle p \hat{\mathbf{z}}; m_n, m_d | v^{\text{PV}} | p \hat{\mathbf{z}}; m_n, m_d \rangle^{(+)} , \quad (2.1)$$

where ρ is the density of deuterons (a parameter under control of the experimenter), v^{PV} denotes the PV nuclear potential, $|p \hat{\mathbf{z}}; m_n, m_d \rangle^{(\mp)}$ are the n - d scattering states with incoming-wave ($-$) and outgoing-wave ($+$) boundary conditions and relative momentum $\mathbf{p} = p \hat{\mathbf{z}}$ taken along the spin-quantization axis, *i.e.* the $\hat{\mathbf{z}}$ -axis, and $v_{\text{rel}} = p/\mu$ is the magnitude of the relative velocity, μ being the n - d reduced mass. The expression above is averaged over the spin projections $m_d = \pm 1, 0$ of the deuteron, however, the phase factor $\epsilon_{m_n} \equiv (-)^{1/2-m_n}$ is ± 1 depending on whether the neutron has $m_n = \pm 1/2$.

The scattering states are calculated from realistic (strong interaction) Hamiltonians including two- and three-nucleon potentials by means of accurate hyperspherical-harmonics techniques [6, 7, 8], and are expanded in partial waves as [14]

$$|p \hat{\mathbf{z}}; m_n m_d \rangle^{(\pm)} = \sqrt{4\pi} \sum_{LSJ} i^L \sqrt{2L+1} \langle 1/2 m_n, 1 m_d | S J_z \rangle \langle S J_z, L 0 | J J_z \rangle |p; LS; J, J_z \rangle^{(\pm)} , \quad (2.2)$$

where

$$|p; LS; J, J_z \rangle^{(\pm)} = \sum_{L'S'} [1 \mp i {}^J R(p)]_{LS, L'S'}^{-1} | \overline{p; L'S'; J, J_z} \rangle . \quad (2.3)$$

In these equations, L denotes the relative orbital angular momentum between the two clusters, S their channel spin (either $1/2$ or $3/2$), and $[{}^J R(p)]_{LS, L'S'}$ is the (real) R -matrix at center-of-mass energy $p^2/(2\mu)$, from which phase-shifts and mixing angles in the channel specified by total angular momentum J are easily obtained. Lastly, the state $| \overline{p; LS; J, J_z} \rangle$ is defined as in Eqs. (2.8) and (2.9) of Ref. [14], and in the asymptotic region (at large n - d separations) reduces to

$$| \overline{p; LS; J, J_z} \rangle \rightarrow \frac{1}{\sqrt{3}} \sum_{ijk \text{ cyclic}} \sum_{L'S'} w_{LS, L'S'}^J(p; y_i) \left[Y_{L'}(\hat{\mathbf{y}}_i) \otimes |i, jk; S' \rangle \right]_J , \quad (2.4)$$

$$w_{LS, L'S'}^J(p; y_i) = \delta_{LL'} \delta_{SS'} j_{L'}(p y_i) + {}^J R_{LS, L'S'}(p) n_{L'}(p y_i) , \quad (2.5)$$

where $|i, jk; S' \rangle$ denotes a state in which neutron i and a deuteron made up of nucleons jk are coupled to channel spin S' , $j_L(x)$ and $n_L(x)$ are, respectively, the regular and irregular spherical Bessel functions, and $\mathbf{y}_i = \mathbf{r}_i - (\mathbf{r}_j + \mathbf{r}_k)/2$ is the n - d vector separation.

We are interested in very low-energy neutrons, and thus it is sufficient to keep only S- and P-wave channels in the partial wave expansion of $|p \hat{\mathbf{z}}; m_n, m_d \rangle^{(\pm)}$. Equation (2.1) is then simply written as

$$\begin{aligned} \frac{1}{\rho} \frac{d\phi}{dz} &= \frac{8\pi}{\sqrt{3} v_{\text{rel}}} \sum_{m_n m_d} \sum_{SJ} \epsilon_{m_n} \langle 1/2 m_n, 1 m_d | J J_z \rangle \langle 1/2 m_n, 1 m_d | S J_z \rangle \\ &\quad \langle S J_z, 1 0 | J J_z \rangle \text{Im} \left[{}^{(-)} \langle p; 1S; J, J_z | v^{\text{PV}} | p; 0J; J, J_z \rangle^{(+)} \right] . \end{aligned} \quad (2.6)$$

The relation above follows by first noting that under time inversions, induced by the antiunitary operator \mathcal{T} , the states in the convention adopted here transform as

$$\mathcal{T} |p; LS; J, J_z\rangle^{(+)} = (-)^{L+J-J_z} |p; LS; J, -J_z\rangle^{(-)}, \quad (2.7)$$

and then using the fact that the PV potential is i) a scalar under rotations (and hence its matrix elements are independent of J_z) and ii) invariant under time inversions, which lead to

$$(-)\langle p; 0J; J, J_z | v^{\text{PV}} | p; 1S; J, J_z \rangle^{(+)} = - (-)\langle p; 1S; J, J_z | v^{\text{PV}} | p; 0J; J, J_z \rangle^{(+)} . \quad (2.8)$$

In Eq. (2.6) the sums over S, J are restricted to $S, J = 1/2$ and $3/2$, and thus the PV potential connects the doublet (quartet) S-wave state ${}^2\text{S}_{1/2}$ (${}^4\text{S}_{3/2}$) to both the doublet and quartet P-wave states ${}^2\text{P}_{1/2}$ (${}^2\text{P}_{3/2}$) and ${}^4\text{P}_{1/2}$ (${}^4\text{P}_{3/2}$). Note that the additional contribution associated with the transition ${}^4\text{S}_{3/2} \rightarrow {}^4\text{F}_{3/2}$ is neglected at the low energies of interest here.

III. THE PARITY-VIOLATING POTENTIAL

Two different models of the PV weak-interaction potentials are adopted in the calculations reported below. One is the model developed almost thirty years ago by Desplanques *et al.* [3] (and known as DDH): it is parameterized in terms of π -, ρ -, and ω -meson exchanges, and involves in principle seven weak pion and vector-meson coupling constants to the nucleon. These were estimated within a quark model approach incorporating symmetry arguments and current algebra requirements [3, 15]. Due to the inherent limitations of such an analysis, however, the coupling constants determined in this way have rather wide ranges of allowed values.

The other model for the PV potential considered in the present work is that formulated in 2005 by Zhu *et al.* [5] within an effective-field-theory (EFT) approach in which only nucleon degrees of freedom are retained explicitly. At lowest order Q/Λ_χ , where Q is the small momentum entering the low-energy PV process and $\Lambda_\chi \simeq 1$ GeV is the scale of chiral symmetry breaking, it is parameterized by a set of twelve contact four-nucleon terms. In fact, it has been recently realized [16] that this set is redundant, and the number of independent contact terms can be reduced to five by Fierz-rearrangement. The derivation is summarized in Appendix A.

The DDH and EFT PV two-nucleon potentials are conveniently written as

$$v_{ij}^\alpha = \sum_{n=1}^{13} c_n^\alpha O_{ij}^{(n)}, \quad \alpha = \text{DDH or EFT}, \quad (3.1)$$

where the parameters c_n^α and operators $O_{ij}^{(n)}$, $n = 1, \dots, 13$, are listed in Table I. In this table the vector operators $\mathbf{X}_{ij,\pm}^{(n)}$ are defined as

$$\mathbf{X}_{ij,+}^{(n)} \equiv [\mathbf{p}_{ij}, f_n(r_{ij})]_+ , \quad (3.2)$$

$$\mathbf{X}_{ij,-}^{(n)} \equiv i [\mathbf{p}_{ij}, f_n(r_{ij})]_- , \quad (3.3)$$

where $[\dots, \dots]_\mp$ denotes the commutator $(-)$ or anticommutator $(+)$, and \mathbf{p}_{ij} is the relative momentum operator, $\mathbf{p}_{ij} \equiv (\mathbf{p}_i - \mathbf{p}_j)/2$. In the DDH model, the functions $f_x(r)$, $x = \pi, \rho$ and ω , are Yukawa functions, suitably modified by the inclusion of monopole form factors,

$$f_x(r) = \frac{1}{4\pi r} \left\{ e^{-m_x r} - e^{-\Lambda_x r} \left[1 + \frac{\Lambda_x r}{2} \left(1 - \frac{m_x^2}{\Lambda_x^2} \right) \right] \right\} . \quad (3.4)$$

In the EFT model, however, the short-distance behavior is described by a single function $f_\mu(r)$, which is itself taken as a Yukawa function with mass parameter μ ,

$$f_\mu(r) = \frac{1}{4\pi r} e^{-\mu r} , \quad (3.5)$$

with $\mu \simeq m_\pi$ as appropriate in the present formulation, in which pion degrees of freedom are integrated out.

In v_{ij}^{DDH} , the strong-interaction coupling constants of the π -, ρ -, and ω -meson to the nucleon are denoted as $g_\pi, g_\rho, \kappa_\rho, g_\omega, \kappa_\omega$, while the weak-interaction ones as $h_\pi^1, h_\pi^0, h_\rho^1, h_\rho^0, h_\omega^2, h_\omega^0, h_\omega^1$, where the superscripts 0, 1, and 2

n	c_n^{DDH}	$f_n^{\text{DDH}}(r)$	c_n^{EFT}	$f_n^{\text{EFT}}(r)$	$O_{ij}^{(n)}$
1	$+\frac{g_\pi h_\pi^1}{2\sqrt{2}m}$	$f_\pi(r)$	$\frac{2\mu^2}{\Lambda_\chi^3} C_6$	$f_\mu(r)$	$(\boldsymbol{\tau}_i \times \boldsymbol{\tau}_j)_z (\boldsymbol{\sigma}_i + \boldsymbol{\sigma}_j) \cdot \mathbf{X}_{ij,-}^{(1)}$
2	$-\frac{g_\rho h_\rho^0}{m}$	$f_\rho(r)$	0	0	$\boldsymbol{\tau}_i \cdot \boldsymbol{\tau}_j (\boldsymbol{\sigma}_i - \boldsymbol{\sigma}_j) \cdot \mathbf{X}_{ij,+}^{(2)}$
3	$-\frac{g_\rho h_\rho^0(1+\kappa_\rho)}{m}$	$f_\rho(r)$	0	0	$\boldsymbol{\tau}_i \cdot \boldsymbol{\tau}_j (\boldsymbol{\sigma}_i \times \boldsymbol{\sigma}_j) \cdot \mathbf{X}_{ij,-}^{(3)}$
4	$-\frac{g_\rho h_\rho^1}{2m}$	$f_\rho(r)$	$\frac{\mu^2}{\Lambda_\chi^3} (C_2 + C_4)$	$f_\mu(r)$	$(\boldsymbol{\tau}_i + \boldsymbol{\tau}_j)_z (\boldsymbol{\sigma}_i - \boldsymbol{\sigma}_j) \cdot \mathbf{X}_{ij,+}^{(4)}$
5	$-\frac{g_\rho h_\rho^1(1+\kappa_\rho)}{2m_2}$	$f_\rho(r)$	0	0	$(\boldsymbol{\tau}_i + \boldsymbol{\tau}_j)_z (\boldsymbol{\sigma}_i \times \boldsymbol{\sigma}_j) \cdot \mathbf{X}_{ij,-}^{(5)}$
6	$-\frac{g_\rho h_\rho^2}{2\sqrt{6}m}$	$f_\rho(r)$	$-\frac{2\mu^2}{\Lambda_\chi^3} C_5$	$f_\mu(r)$	$(3\tau_{i,z}\tau_{j,z} - \boldsymbol{\tau}_i \cdot \boldsymbol{\tau}_j) (\boldsymbol{\sigma}_i - \boldsymbol{\sigma}_j) \cdot \mathbf{X}_{ij,+}^{(6)}$
7	$-\frac{g_\rho h_\rho^2(1+\kappa_\rho)}{2\sqrt{6}m}$	$f_\rho(r)$	0	0	$(3\tau_{i,z}\tau_{j,z} - \boldsymbol{\tau}_i \cdot \boldsymbol{\tau}_j) (\boldsymbol{\sigma}_i \times \boldsymbol{\sigma}_j) \cdot \mathbf{X}_{ij,-}^{(7)}$
8	$-\frac{g_\omega h_\omega^0}{m}$	$f_\omega(r)$	$\frac{2\mu^2}{\Lambda_\chi^3} C_1$	$f_\mu(r)$	$(\boldsymbol{\sigma}_i - \boldsymbol{\sigma}_j) \cdot \mathbf{X}_{ij,+}^{(8)}$
9	$-\frac{g_\omega h_\omega^0(1+\kappa_\omega)}{m}$	$f_\omega(r)$	$\frac{2\mu^2}{\Lambda_\chi^3} \tilde{C}_1$	$f_\mu(r)$	$(\boldsymbol{\sigma}_i \times \boldsymbol{\sigma}_j) \cdot \mathbf{X}_{ij,-}^{(9)}$
10	$-\frac{g_\omega h_\omega^1}{2m}$	$f_\omega(r)$	0	0	$(\boldsymbol{\tau}_i + \boldsymbol{\tau}_j)_z (\boldsymbol{\sigma}_i - \boldsymbol{\sigma}_j) \cdot \mathbf{X}_{ij,+}^{(10)}$
11	$-\frac{g_\omega h_\omega^1(1+\kappa_\omega)}{2m}$	$f_\omega(r)$	0	0	$(\boldsymbol{\tau}_i + \boldsymbol{\tau}_j)_z (\boldsymbol{\sigma}_i \times \boldsymbol{\sigma}_j) \cdot \mathbf{X}_{ij,-}^{(11)}$
12	$-\frac{g_\omega h_\omega^1 - g_\rho h_\rho^1}{2m}$	$f_\rho(r)$	0	0	$(\boldsymbol{\tau}_i - \boldsymbol{\tau}_j)_z (\boldsymbol{\sigma}_i + \boldsymbol{\sigma}_j) \cdot \mathbf{X}_{ij,+}^{(12)}$
13	$-\frac{g_\rho h_\rho^1}{2m}$	$f_\rho(r)$	0	0	$(\boldsymbol{\tau}_i \times \boldsymbol{\tau}_j)_z (\boldsymbol{\sigma}_i + \boldsymbol{\sigma}_j) \cdot \mathbf{X}_{ij,-}^{(13)}$

TABLE I: Components of the DDH and EFT models for the parity-violating potential. The vector operators $\mathbf{X}_{ij,\mp}^{(n)}$ and functions $f_x(r)$, $x = \pi, \rho, \omega, \mu$, are defined in Eqs. (3.2)–(3.3) and Eqs. (3.4)–(3.5), respectively. As outlined in the Appendix A, only 5 operators and low-energy constants enter the pionless EFT interaction at the leading order, and in this paper they have been chosen to correspond to the rows 1, 4, 6, 8 and 9. .

specify the isoscalar, isovector, and isotensor content of the corresponding interactions. In the EFT model, the five low-energy constants $C_1, \tilde{C}_1, C_2 + C_4, C_5$ and C_6 completely characterize v_{ij}^{EFT} , to lowest order Q/Λ_χ (see Appendix A).

In the analysis of the neutron spin-rotation observable to follow, we will report results for the coefficients I_n^{DDH} and I_n^{EFT} in the expansion

$$\frac{1}{\rho} \frac{d\phi}{dz} = \sum_{n=1}^{13} c_n^\alpha I_n^\alpha. \quad (3.6)$$

Thus we will not need to consider specific values, or rather range of values, for the strength parameters c_n^α . However, the I_n^α depend on the masses (and short-range cutoffs Λ_x for the DDH model) occurring in the Yukawa functions. Two different sets of values are used for Λ_x and μ in the present study, as listed in Table II. Both were used in the DDH-based calculations of PV two-nucleon observables in Refs. [1, 2].

IV. CALCULATION

The relevant matrix elements which need to be calculated in Eq. (2.6) are given by

$$\langle p; 1S; J, J_z | v^{\text{PV}} | p; 0J; J, J_z \rangle^{(+)} = 3 \int d\mathbf{x} d\mathbf{y} \left[\psi_{1S;JJ_z}^{(-)}(\mathbf{x}, \mathbf{y}) \right]^\dagger v_{23}^\alpha \psi_{0J;JJ_z}^{(+)}(\mathbf{x}, \mathbf{y}), \quad (4.1)$$

where $\mathbf{x} \equiv \mathbf{r}_2 - \mathbf{r}_3$ and $\mathbf{y} \equiv \mathbf{r}_1 - (\mathbf{r}_2 + \mathbf{r}_3)/2$ is the n -d vector separation defined earlier. The factor of 3 on the right-hand-side simply accounts for the three identical contributions associated with the sum over pairs included in

	Λ_π	Λ_ρ	Λ_ω		μ
DDH-I	1.72	1.31	1.50	EFT-I	0.138
DDH-II	∞	∞	∞	EFT-II	1.0

TABLE II: The two different sets of values, in GeV units, for the short-range cutoffs Λ_x (mass μ) used in the DDH (EFT) model. Note that the masses m_π , m_ρ , and m_ω are taken respectively as 0.138, 0.771, and 0.783 in units of GeV. The row with $\Lambda_x = \infty$ corresponds to point-like couplings.

v^{PV} ,

$$v^{\text{PV}} = \sum_{i < j} v_{ij}^{\alpha} , \quad (4.2)$$

where $\alpha = \text{DDH}$ or EFT .

The (antisymmetric) wave functions $\psi(\mathbf{x}, \mathbf{y})$, dropping subscripts and superscripts for brevity, are written as

$$\psi(\mathbf{x}, \mathbf{y}) = \sum_{ijk \text{ cyclic}} \psi_{i,jk}(\mathbf{x}_i, \mathbf{y}_i) , \quad (4.3)$$

where

$$\mathbf{x}_i = \mathbf{r}_j - \mathbf{r}_k , \quad \mathbf{y}_i = \mathbf{r}_i - (\mathbf{r}_j + \mathbf{r}_k)/2 , \quad (4.4)$$

$(ijk) = (123)$, (231) , and (312) are the three cyclic permutations of the particles, and $\mathbf{x}_1 \equiv \mathbf{x}$ and $\mathbf{y}_1 \equiv \mathbf{y}$. The decomposition given in Eq. (4.3) corresponds to the three possible partitions of three nucleons in 1+2 clusters—indeed, the asymptotic wave functions in Eq. (2.4) have precisely this form. Note that in the integral of Eq. (4.1) there are terms like (again in a schematic notation)

$$\int d\mathbf{x} d\mathbf{y} \psi_{1;23}^{\dagger}(\mathbf{x}_1, \mathbf{y}_1) v_{23}^{\alpha} \psi_{1;23}(\mathbf{x}_1, \mathbf{y}_1) , \quad (4.5)$$

corresponding to the partition nucleon 1 and nucleons 23 in the initial and final n - d states, and with the PV interaction acting on nucleons 23. These n - d continuum wave functions have “core” parts which vanish at ∞ , and asymptotic parts oscillating in the y_1 variable. The integrals involving core parts of either the left or right (or both) wave functions are converging, while the integral involving the left and right asymptotic wave functions vanishes, since the integrand is odd under inversion $\mathbf{y}_1 \rightarrow -\mathbf{y}_1$. The remaining partitions give converging contributions to the integral, since the deuteron cluster in the left and right wave functions is made up of different nucleons and $\psi_{2;31}(\mathbf{x}_2, \mathbf{y}_2)$, $\psi_{3;12}(\mathbf{x}_3, \mathbf{y}_3) \rightarrow 0$ as $\mathbf{y}_1 \rightarrow \infty$.

The wave functions for an assigned spatial configuration (\mathbf{x}, \mathbf{y}) are expanded on a basis of 8×3 spin-isospin states for the three nucleons as

$$\psi(\mathbf{x}, \mathbf{y}) = \sum_{a=1}^{24} \psi_a(\mathbf{x}, \mathbf{y}) |a\rangle , \quad (4.6)$$

where the components $\psi_a(\mathbf{x}, \mathbf{y})$ are generally complex functions, and the basis states $|a\rangle = |(n \downarrow)_1 (p \downarrow)_2 (n \downarrow)_3\rangle$, $|(n \downarrow)_1 (n \downarrow)_2 (p \downarrow)_3\rangle$, and so on. Matrix elements of the PV potential components are written schematically as

$$\langle f | O | i \rangle = \sum_{a,b=1}^{24} \int d\mathbf{x} d\mathbf{y} \psi_{f,a}^*(\mathbf{x}, \mathbf{y}) [O(\mathbf{x})]_{ab} \psi_{i,b}(\mathbf{x}, \mathbf{y}) , \quad (4.7)$$

where $[O(\mathbf{x})]_{ab}$ denotes the matrix representing in configuration space any of the components in Table I. Note that the operators $\mathbf{X}_{23,\mp}^{(n)}$ occurring in v_{23}^{α} are conveniently expressed as

$$\mathbf{X}_{23,-}^{(n)} = \hat{\mathbf{x}} f'_n(x) , \quad \mathbf{X}_{23,+}^{(n)} = -i [2 f_n(x) \nabla_x + \hat{\mathbf{x}} f'_n(x)] , \quad (4.8)$$

where the gradient operator $\nabla_x = (\nabla_2 - \nabla_3)/2$ acts on the right (initial) wave function, and $f'(x) = df(x)/dx$. Gradients are discretized as

$$\nabla_{i,\alpha} \psi(\mathbf{x}, \mathbf{y}) \simeq \frac{\psi(\dots \mathbf{r}_i + \delta \hat{\mathbf{e}}_{\alpha} \dots) - \psi(\dots \mathbf{r}_i - \delta \hat{\mathbf{e}}_{\alpha} \dots)}{2\delta} , \quad (4.9)$$

where δ is a small increment and $\hat{\mathbf{e}}_{\alpha}$ is a unit vector in the α -direction. Matrix multiplications in the spin-isospin space are performed exactly with the techniques developed in Ref. [17]. The problem is then reduced to the evaluation of the spatial integrals, which is efficiently carried out by a combination of Monte Carlo (MC) and standard quadratures techniques. We write

$$\langle f | O | i \rangle = \int d\hat{\mathbf{x}} d\hat{\mathbf{y}} F(\hat{\mathbf{x}}, \hat{\mathbf{y}}) \simeq \frac{1}{N_c} \sum_{c=1}^{N_c} F(c) , \quad (4.10)$$

where the c 's denote uniformly sampled directions $(\hat{\mathbf{x}}, \hat{\mathbf{y}})$ (total number N_c). For each such configuration c , the function F is obtained by Gaussian integrations over the x and y variables, *i.e.*

$$F(c) = (4\pi)^2 \sum_{a,b=1}^{24} \int_0^\infty dx x^2 \int_0^\infty dy y^2 \psi_{f,a}^*(\mathbf{x}, \mathbf{y}) [O(\mathbf{x})]_{ab} \psi_{i,b}(\mathbf{x}, \mathbf{y}) . \quad (4.11)$$

Convergence in the x and y integrations requires of the order of 40 Gaussian points, distributed over a non-uniform grid extending beyond 40 fm, while N_c of the order of a few thousands is sufficient to reduce the statistical error in the MC integration at the percent level. Thus, the present method turns out to be computationally intensive. In this respect, we note that a direct MC evaluation of the six-dimensional integral in Eq. (4.7) by Metropolis sampling from a probability density function $W(\mathbf{x}, \mathbf{y}) \propto |\psi_0(\mathbf{x}, \mathbf{y})|^2$, where ψ_0 is the triton bound-state wave function, turned out to be impractical. This was also the case for other choices of W , such as $W(\mathbf{x}, \mathbf{y}) \propto x^\lambda y^\nu |\phi(\mathbf{x})|^2 |\phi(\mathbf{y})|^2$, where ϕ is the deuteron wave function. The reason for this difficulty can be appreciated by examining Fig. 1, in which the integrand associated with the pion-range component of the DDH potential, specifically the matrix element of $O^{(1)}$ between the $^2S_{1/2}$ and $^2P_{1/2}$ n - d states at zero energy, is plotted as function of the hyper-radius $\rho = \sqrt{x^2 + 4y^2/3}$. Note the change of sign in this function, due to the node in the continuum $^2S_{1/2}$ state (thus ensuring its orthogonality to the 3H bound state), and its long-range character. This last feature, in particular, makes it difficult for an efficient sampling of the large ρ region with the importance functions W mentioned above.

The computer codes were successfully tested by carrying out a calculation based on Gaussian wave functions for the initial and final states, as described in the following subsection.

A. Test calculation

We have performed calculations with Gaussian-type wave functions, for which the matrix elements can be computed analytically. In Eq. (4.1), we have replaced the realistic n - d wave functions with the following ones

$$\tilde{\psi}_{LS;JJ_z}(\mathbf{x}, \mathbf{y}) = \frac{\exp(-\beta \rho^2)}{\sqrt{4\pi}} \Omega_{LS;JJ_z} , \quad (4.12)$$

with

$$\Omega_{LS;JJ_z} = \sum_{ijk \text{ cyclic}} y_i^L F_{LSJ}(y_i) \left[Y_L(\hat{\mathbf{y}}_i) \otimes [s_i S_{jk}]_S \right]_{JJ_z} [t_i T_{jk}]_{TT_z} , \quad (4.13)$$

where ρ is the hyper-radius (independent of the particle permutation considered), s_i (t_i) denotes the spin (isospin) state of particle i , and S_{jk} (T_{jk}) the spin (isospin) state of particles jk . We have considered only states of total isospin $T, T_z=1/2, -1/2$, appropriate to describe the n - d channel—possible admixtures of $T=3/2$ components induced by isospin symmetry breaking terms in the strong and electromagnetic interactions are expected to give negligible contributions to PV observables.

The quantum numbers S_{jk} and T_{jk} are respectively taken to be 1 and 0, while the factors $F_{LSJ}(y_i)$ selected for the various channels are reported in Table III. Note that $F_{LSJ}(y_i)=1$ except for $L=0$ and $S=J=3/2$, since in this case the spin part $[s_i S_{jk}]_{3/2}$ is totally symmetric, and it is impossible to construct a fully antisymmetric wave function with only the isospin part. Hence, the choice $F(y_i)=y_i^2$. In all other channels, non-vanishing functions $\Omega_{LS;JJ_z}$ are obtained by simply taking $F_{LSJ}(y_i)=1$.

The analytical calculation is simplified considerably by expressing the function $\Omega_{LS;JJ_z}$, which involves the three set of coordinates $(\mathbf{x}_1, \mathbf{y}_1)$, $(\mathbf{x}_2, \mathbf{y}_2)$, and $(\mathbf{x}_3, \mathbf{y}_3)$ corresponding to the three partitions (1,23), (2,31), and (3,12), in

L	S	J	$F_{LSJ}(y_i)$
0	1	1	1
0	3/2	3/2	y_i^2
1	1	1	1
1	3/2	3/2	1
1	3/2	5/2	1
1	3/2	5/2	1
1	3/2	5/2	1

TABLE III: Quantum numbers and factor $F_{LSJ}(y_i)$ entering the Gaussian wave functions given in Eq. (4.12).

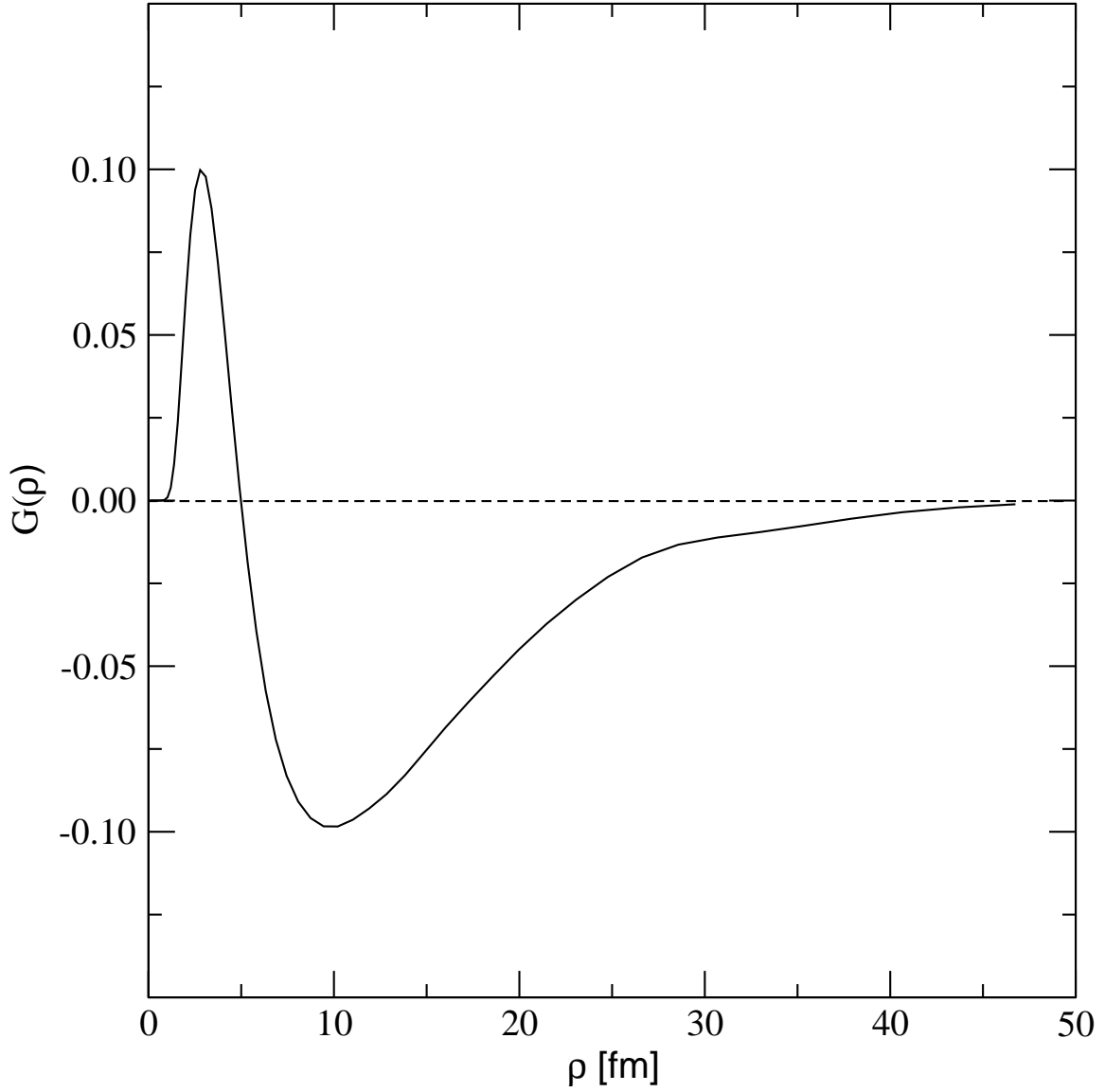


FIG. 1: The function $G(\rho)$, defined so that $\int_0^\infty d\rho G(\rho)$ is the matrix element of the operator $O^{(1)}$ between the $^2S_{1/2}$ and $^2P_{1/2}$ n - d states at zero energy, plotted as function of the hyper-radius $\rho = \sqrt{x^2 + 4y^2/3}$.

terms of linear combinations of functions of, say, the first set of spatial variables, *i.e.* $\mathbf{x} \equiv \mathbf{x}_1$ and $\mathbf{y} \equiv \mathbf{y}_1$ as in Eq. (4.1), and spin-isospin states of pair 23 only. We find:

$$\Omega_{LS;JJ_z} = \sum_{n_x, n_y, \ell_x, S_x, j_x, \ell_y, j_y, T_x} c_{n_x, n_y, \ell_x, S_x, j_x, \ell_y, j_y, T_x}^{LSJ} \Omega_{n_x, n_y, \ell_x, S_x, j_x, \ell_y, j_y, T_x}^{JJ_z; TT_z} \quad (4.14)$$

where

$$\Omega_{n_x, n_y, \ell_x, S_x, j_x, \ell_y, j_y, T_x}^{JJ_z; TT_z} = x^{\ell_x + n_x} y^{\ell_y + n_y} \left[[Y_{\ell_x}(\hat{\mathbf{x}}) S_x]_{j_x} \otimes [Y_{\ell_y}(\hat{\mathbf{y}}) s_1]_{j_y} \right]_{JJ_z} [T_x t_1]_{TT_z} \quad (4.15)$$

and n_x and n_y are non-negative integers, S_x and T_x are the spin and isospin states of pair 23, and $c_{n_x, n_y, \ell_x, S_x, j_x, \ell_y, j_y, T_x}^{LSJ}$ are numerical factors, which can easily be expressed in terms of Wigner coefficients.

It is now relatively simple to compute matrix elements of the operators $O_{23}^{(n)}$ in Table I between states

$\Omega_{n_x, n_y, \ell_x, S_x, j_x, \ell_y, j_y, T_x}^{JJ_z; TT_z}$ by making use of the following relations

$$\int d\hat{\mathbf{x}} [Y_{\ell_x}(\hat{\mathbf{x}})S_x]_{j_x m_x}^\dagger (\boldsymbol{\sigma}_2 + \boldsymbol{\sigma}_3) \cdot \hat{\mathbf{x}} [Y_{\ell'_x}(\hat{\mathbf{x}})S'_x]_{j_x m_x} = -2\sqrt{\frac{j_x + 1/2 \pm 1/2}{2j_x + 1}} \delta_{\ell_x, j_x} \delta_{S_x, 1} \delta_{S'_x, 1} \delta_{\ell'_x, j_x \mp 1}, \quad (4.16)$$

and similar ones for the spin-space and isospin operators occurring in the potential components $O_{23}^{(n)}$. In particular, those for $(\boldsymbol{\sigma}_2 - \boldsymbol{\sigma}_3) \cdot \nabla_x$ and $(\boldsymbol{\sigma}_2 \times \boldsymbol{\sigma}_3) \cdot \hat{\mathbf{x}}$ are listed in Sec. III.E of Ref. [1]. The remaining task of integrating over the radial variables x and y is carried out accurately by means of Gauss quadrature formulae.

The results of the “analytical” calculation just described are found to be in agreement, for each of the 13 components of the PV potential, with those produced by a MC calculation using the same input wave functions as in Eq. (4.12). The spin-isospin algebra is performed as outlined in the previous section; however, because of the short-range character of the wave functions in this case, spatial configurations turn out to be efficiently sampled with the Metropolis algorithm by a probability density proportional to $\exp(-2\beta\rho^2)$. In a typical calculation, the values $\beta = 0.10\text{--}0.25 \text{ fm}^{-2}$ have been selected.

V. RESULTS AND CONCLUSIONS

The results for the coefficients I_n^α in Eq. (3.6), obtained with n - d continuum wave functions corresponding to the AV18 and AV18/UIX strong-interaction Hamiltonians, are reported for the DDH and pionless EFT PV potentials in Tables IV and V, respectively. The labels I and II for the columns in each of these tables refer to the two sets of cutoff parameters, as given in Table II. The subscript n in I_n^α specifies the operators as listed in Table I. Note that results for $n=13$ are not reported, since the coupling constant $h_\rho^{1'}$ multiplying these contributions has been estimated to be considerably smaller [15] than the “best” values estimated for the other coupling constants in the original DDH reference [3].

n	DDH-I		DDH-II	
	AV18	AV18/UIX	AV18	AV18/UIX
1	0.256E+03	0.270E+03	0.257E+03	0.274E+03
2	-0.444E+01	-0.691E+01	-0.719E+01	-0.118E+02
3	0.444E+01	0.401E+01	0.732E+01	0.761E+01
4	-0.231E+01	-0.881E+00	-0.332E+01	-0.148E+01
5	-0.247E+01	-0.122E+01	-0.387E+01	-0.234E+01
8	0.420E+01	0.362E+01	0.543E+01	0.516E+01
9	0.111E+01	-0.117E+00	0.136E+01	-0.189E+00
10	-0.253E+01	-0.991E+00	-0.314E+01	-0.141E+01
11	-0.280E+01	-0.144E+01	-0.369E+01	-0.225E+01
12	0.316E+01	0.339E+01	0.455E+01	0.546E+01

TABLE IV: The coefficients I_n^{DDH} (in fm) in Eq. (3.6) corresponding to the DDH PV potential in combination with the AV18 and AV18/UIX strong-interaction potentials for the two different sets of cutoff parameters given in Table II. The statistical errors associated with the Monte Carlo integrations are not shown, but are typically at the 1-2% level. Note that the coefficients $I_{n=6,7}^{\text{DDH}}$ vanish because of isospin selection rules.

A quick glance at Table IV makes it clear that the matrix element of the long-range component of the DDH potential due to pion exchange is almost two orders of magnitude larger than that of its short-range components induced by vector-meson exchanges. It is also clear that this contribution is fairly insensitive to the choice of cutoffs as well as of input strong-interaction Hamiltonians used to generate the n - d S- and P-wave channel states. In particular, one should note that the AV18 and AV18/UIX models predict rather different values for the scattering length in the $^2\text{S}_{1/2}$ channel [8]. On the other hand, predictions for the $^4\text{S}_{1/2}$ scattering length are very close to each other. This is reflected in the contributions to I_1^{DDH} due to the doublet and quartet S-wave channels. We find that for the case of DDH-I, for example, these contributions for the AV18 and AV18/UIX are, respectively, 45.0 fm and 74.2 fm in the $^2\text{S}_{1/2}$ channel, and 210.6 fm and 196.6 fm in the $^4\text{S}_{1/2}$ channel, which add up (up to truncation errors) to the values 256 fm and 270 fm, reported in the first row of Table IV. We observe that the doublet scattering length calculated with the AV18/UIX is very close to the experimental determination of this quantity, while the quartet scattering length, which is much less sensitive to the presence of three-nucleon interactions, is found to be in agreement with the experimental value with both the AV18 and AV18/UIX models. Hence, it is reasonable to expect that any strong-interaction Hamiltonian

that reproduces the experimental scattering lengths should lead to predictions for the long-range component of the DDH potential, which are very similar to those reported here for the AV18/UIX model.

There is considerable model dependence in the results obtained for the individual contributions due to vector-meson exchanges. However, this model dependence has little impact on the neutron spin rotation, as it can be surmised from Table VI, where we list predictions obtained for this observable. We adopt two different sets of strong- and weak-interaction coupling constants, namely those reported in Tables I and II of Ref. [2]. The set of coupling constants denoted as DDH-best (from Table II of Ref. [2]) is the “best value” set as given in the original work [3]. Recently, the ρ - and ω -meson weak-coupling constants were adjusted in Ref. [1] to reproduce precise measurements of the longitudinal asymmetry in \vec{p} - p elastic scattering (see Table I of Ref. [2]). The resulting set of coupling constants is denoted as DDH-adj. Note that both sets use $h_\pi^1 = 4.56 \times 10^{-7}$. Assuming a liquid deuterium density of $\rho = 0.4 \times 10^{23}$ atoms cm^{-3} , we obtain $d\phi/dz \approx 0.53 \times 10^{-7}$ rad-cm $^{-1}$ (0.56×10^{-7} rad-cm $^{-1}$) with the AV18/UIX+DDH-best (AV18/UIX+DDH-adj) model. About 90% of this prediction comes from the long-range component of DDH, while its short-range components contribute the remaining 10%. In particular, the reason for the larger short-range contribution obtained with DDH-adj relative to DDH-best lies in the fact that this contribution is dominated by the $n = 3$ term in Eq. (3.6), for which the combination of coupling constants is $c_3 = -g_\rho h_\rho^0 (1 + \kappa_\rho)/m$ (see Table I). In DDH-adj c_3 is roughly a factor of two larger than in DDH-best because of different values for h_ρ^0 and the tensor coupling constant κ_ρ .

It is interesting to note that the neutron spin rotation in \vec{n} - p scattering is predicted to be about one order of magnitude smaller than in the present case [2], which should make its measurement in \vec{n} - d scattering considerably easier, at least in principle.

n	EFT-I		EFT-II	
	AV18	AV18/UIX	AV18	AV18/UIX
1	0.257E+03	0.274E+03	0.392E+01	0.706E+01
4	-0.154E+03	-0.508E+02	-0.127E+01	-0.682E+00
8	0.260E+03	0.189E+03	0.233E+01	0.251E+01
9	0.244E+00	-0.359E+02	0.557E+00	-0.955E-01

TABLE V: Same as in Table IV but for the pionless EFT PV potential. Note that there are no potential components with $O_{ij}^{(n)}$ with $n=2, 3, 5, 7, 10$ and 11 , and that the coefficient $I_{n=6}^{\text{EFT}}$ vanishes because of isospin selection rules.

The coefficients I_n^{EFT} for the relevant operators entering the pionless EFT PV potential, that is $n=1, 4, 6, 8$, and 9 , are reported in Table V. Note that the $n=6$ operator is isotensor, and therefore its matrix element vanishes here. The I_n^{EFT} coefficients are all of the same order of magnitude, since the radial functions are taken to be the same for all n , $f_n^{\text{EFT}}(r) = f_\mu(r)$. Of course, they depend significantly on the value of the mass μ —either $\mu = m_\pi$ (EFT-I), as appropriate in the present pionless EFT formulation, or $\mu = 1$ GeV (EFT-II), the scale of chiral symmetry breaking, as appropriate in the formulation in which pion degrees of freedom are explicitly retained. Indeed, in this latter formulation the leading order component of v^{PV} has the same form as the pion-exchange term in DDH.

We note that the coefficient $I_{n=1}^{\text{EFT}}$ is weakly dependent on the choice of input strong-interaction Hamiltonian—AV18 or AV18/UIX—in the case of the EFT-I model. On the other hand, this is not the case for the $I_{n=4,8,9}^{\text{EFT}}$ coefficients.

Finally, rough estimates have been made for the range of values allowed for the low-energy constants $C_1, C_2 + C_4, C_5, \tilde{C}_1$, and C_6 in Ref. [5]. However, at the present time a systematic program for their determination is yet to be carried out. In view of this, we refrain here from making EFT-based predictions for the spin rotation observable.

	AV18		AV18/UIX	
	DDH-best	DDH-adj	DDH-best	DDH-adj
π	0.457	0.457	0.485	0.485
ρ - ω	0.063	0.092	0.046	0.075
TOT	0.520	0.550	0.531	0.560

TABLE VI: Spin rotation for \vec{n} - d scattering in units of 10^{-7} rad-cm $^{-1}$ at zero energy, obtained for the DDH-I model assuming a liquid deuterium density of $\rho = 0.4 \times 10^{23}$ atoms cm^{-3} . The columns labeled DDH-best (DDH-adj) list the spin rotation predicted using the “best” (“adjusted”) values for the weak-interaction coupling constants, as reported in Table II (I) of Ref. [2]. The row labeled “ π ” (“ ρ - ω ”) lists the results obtained by including only the pion (ρ and ω mesons), while that labeled “TOT” gives the total contributions.

In conclusion, we have calculated the neutron spin rotation, induced by PV components in the nucleon-nucleon potential, in \vec{n} - d scattering at zero energy. We find that this observable is dominated by the contribution of the long-range part of the PV potential due to pion exchange, and that the model-dependence of this contribution is weak. The

predicted $d\phi/dz$ is $\simeq 0.5 \times 10^{-7}$ rad-cm $^{-1}$ —an order of magnitude larger than expected in \bar{n} - p scattering [2]. Thus a measurement of the spin rotation in \bar{n} - d scattering could provide a further constraint, complementary to that coming from measurements of the photon asymmetry in \bar{n} - p radiative capture, on the strength of the long-range component of the hadronic weak interaction.

Acknowledgments

We would like to thank D. Markoff for her interest in the present work. One of the authors (R.S.) would also like to thank the Physics Department of the University of Pisa for the support and warm hospitality extended to him on several occasions.

The work of R.S. is supported by the U.S. Department of Energy under contract DE-AC05-06R23177. The calculations were made possible by grants of computing time from the National Energy Research Supercomputer Center.

APPENDIX A

The leading order PV contact Lagrangian has been written in Ref. [5] as consisting of twelve operators,

$$\mathcal{L} = \sum_{i=1}^6 (C_i O_i + \tilde{C}_i \tilde{O}_i) , \quad (\text{A1})$$

where

$$\begin{aligned} O_1 &= \bar{\psi} 1 \gamma^\mu \psi \bar{\psi} 1 \gamma_\mu \gamma_5 \psi , & \tilde{O}_1 &= \bar{\psi} 1 \gamma^\mu \gamma_5 \psi \partial^\nu (\bar{\psi} 1 \sigma_{\mu\nu} \psi) , \\ O_2 &= \bar{\psi} 1 \gamma^\mu \psi \bar{\psi} \tau_3 \gamma_\mu \gamma_5 \psi , & \tilde{O}_2 &= \bar{\psi} 1 \gamma^\mu \gamma_5 \psi \partial^\nu (\bar{\psi} \tau_3 \sigma_{\mu\nu} \psi) , \\ O_3 &= \bar{\psi} \tau^a \gamma^\mu \psi \bar{\psi} \tau^a \gamma_\mu \gamma_5 \psi , & \tilde{O}_3 &= \bar{\psi} \tau^a \gamma^\mu \gamma_5 \psi \partial^\nu (\bar{\psi} \tau^a \sigma_{\mu\nu} \psi) , \\ O_4 &= \bar{\psi} \tau_3 \gamma^\mu \psi \bar{\psi} 1 \gamma_\mu \gamma_5 \psi , & \tilde{O}_4 &= \bar{\psi} \tau_3 \gamma^\mu \gamma_5 \psi \partial^\nu (\bar{\psi} 1 \sigma_{\mu\nu} \psi) , \\ O_5 &= \mathcal{I}_{ab} \bar{\psi} \tau^a \gamma^\mu \psi \bar{\psi} \tau^b \gamma_\mu \gamma_5 \psi , & \tilde{O}_5 &= \mathcal{I}_{ab} \bar{\psi} \tau^a \gamma^\mu \gamma_5 \psi \partial^\nu (\bar{\psi} \tau^b \sigma_{\mu\nu} \psi) , \\ O_6 &= i \epsilon^{ab3} \bar{\psi} \tau^a \psi \bar{\psi} \tau^b \gamma_5 \psi , & \tilde{O}_6 &= i \epsilon^{ab3} \bar{\psi} \tau^a \gamma^\mu \psi \partial^\nu (\bar{\psi} \tau^b \sigma_{\mu\nu} \gamma_5 \psi) , \end{aligned} \quad (\text{A2})$$

where the nucleon field ψ is a doublet in isospin space, and the operators 1 and τ^a above act on this space. In addition, \mathcal{I}_{ab} is a 3×3 diagonal matrix with elements (1, 1, -2). Using Fierz transformations and fields' equations of motion, the following relations may be shown to hold [16],

$$\begin{aligned} O_3 &= O_1 , \\ O_2 - O_4 &= 2O_6 , \\ \tilde{O}_3 &= 2m(O_1 + O_3) - 3\tilde{O}_1 , \\ \tilde{O}_2 + \tilde{O}_4 &= m(O_2 + O_4) , \\ \tilde{O}_2 - \tilde{O}_4 &= -2mO_6 - \tilde{O}_6 , \\ \tilde{O}_5 &= O_5 , \end{aligned} \quad (\text{A3})$$

so that the number of independent operators can be reduced to six. Moreover, since the relativistic operators O_6 and \tilde{O}_6 give rise to the same structure in the leading order of the non-relativistic expansion, as already observed in Ref. [5], the PV two-nucleon non-relativistic contact Lagrangian consists of only five operators,

$$\begin{aligned} \mathcal{L}_{PV,NN} &= \frac{1}{\Lambda_\chi^3} \left\{ C_1 (N^\dagger \vec{\sigma} N \cdot N^\dagger i \overleftrightarrow{\nabla} N - N^\dagger N N^\dagger i \overleftrightarrow{\nabla} \cdot \vec{\sigma} N) - \tilde{C}_1 \epsilon_{ijk} N^\dagger \sigma^i N \nabla^j (N^\dagger \sigma^k N) \right. \\ &\quad - (C_2 + C_4) \epsilon_{ijk} [N^\dagger \tau_3 \sigma^i N \nabla^j (N^\dagger \sigma^k N) + N^\dagger \sigma^i N \nabla^j (N^\dagger \tau_3 \sigma^k N)] \\ &\quad \left. - \tilde{C}_5 \mathcal{I}_{ab} \epsilon_{ijk} N^\dagger \tau^a \sigma^i N \nabla^j (N^\dagger \tau^b \sigma^k N) + C_6 \epsilon^{ab3} \vec{\nabla} (N^\dagger \tau^a N) \cdot N^\dagger \tau^b \vec{\sigma} N \right\} , \end{aligned} \quad (\text{A4})$$

where the notations of Ref. [5] have been chosen for the coupling constants. Accordingly, the pionless EFT potential in coordinate space reads as

$$\begin{aligned} v_{ij}^{\text{EFT}} &= \frac{2\mu^2}{\Lambda_\chi^3} \left\{ \left[C_1 + (C_2 + C_4) \left(\frac{\tau_i + \tau_j}{2} \right)_z + C_5 \mathcal{I}_{ab} \tau_i^a \tau_j^b \right] (\boldsymbol{\sigma}_i - \boldsymbol{\sigma}_j) \cdot [\mathbf{p}_{ij} , f_\mu(r)]_+ \right. \\ &\quad \left. + i \tilde{C}_1 (\boldsymbol{\sigma}_i \times \boldsymbol{\sigma}_j) \cdot [\mathbf{p}_{ij} , f_\mu(r)]_- + i C_6 \epsilon^{ab3} \tau_i^a \tau_j^b (\boldsymbol{\sigma}_i + \boldsymbol{\sigma}_j) \cdot [\mathbf{p}_{ij} , f_\mu(r)]_- \right\} , \end{aligned}$$

where \mathbf{p}_{ij} is the relative momentum operator and $f_\mu(r)$, defined in Eq. (3.5), is introduced to regularize the potential at short-range.

-
- [1] J. Carlson, R. Schiavilla, V.R. Brown, and B.F. Gibson, Phys. Rev. C **65**, 035502 (2002).
 - [2] R. Schiavilla, J. Carlson, and M. Paris, Phys. Rev. C **70**, 044007 (2004).
 - [3] B. Desplanques, J.F. Donoghue, B.R. Holstein, Ann. Phys. (N.Y.) **124**, 449 (1980).
 - [4] M.J. Ramsey-Musolf and S.A. Page, Ann. Rev. Nucl. Part. Sci. **56**, 1 (2006).
 - [5] S.-L. Zhu, C.M. Maekawa, B.R. Holstein, M.J. Ramsey-Musolf, and U. van Kolck, Nucl. Phys. **A748**, 435 (2005).
 - [6] A. Kievsky, S. Rosati, and M. Viviani, Nucl. Phys. **A577**, 511 (1994)
 - [7] A. Kievsky, M. Viviani, and L.E. Marcucci, Phys. Rev. **C69**, 014002 (2004)
 - [8] A. Kievsky, S. Rosati, M. Viviani, L.E. Marcucci, and L. Girlanda, J. Phys. G **35**, 063101 (2008)
 - [9] R.B. Wiringa, V.G.J. Stoks, and R. Schiavilla, Phys. Rev. C **51**, 38 (1995).
 - [10] B.S. Pudliner *et al.*, Phys. Rev. Lett. **74**, 4396 (1995).
 - [11] J. Carlson and R. Schiavilla, Rev. Mod. Phys. **70**, 743 (1998).
 - [12] L.E. Marcucci, K.M. Nollett, R. Schiavilla, and R.B. Wiringa, Nucl. Phys. **A777**, 111 (2006).
 - [13] E. Fermi, *Nuclear Physics* (The University of Chicago Press, Chicago, 1950).
 - [14] M. Viviani, R. Schiavilla, and A. Kievsky, Phys. Rev. C **54**, 534 (1996).
 - [15] B.R. Holstein, Phys. Rev. D **23**, 1618 (1981).
 - [16] L. Girlanda, arXiv:0804.0772.
 - [17] R. Schiavilla, V.R. Pandharipande, and D.O. Riska, Phys. Rev. C **40**, 2294 (1989).